Evidence for the role of the magnon energy relaxation length in the spin Seebeck effect

Arati Prakash, Benedetta Flebus, Jack Brangham, Fengyuan Yang, Yaroslav Tserkovnyak, and Joseph P. Heremans

Phys. Rev. B **97**, 020408 — Published 29 January 2018

DOI: 10.1103/PhysRevB.97.020408

Evidence for the role of the magnon energy relaxation length in the Spin Seebeck Effect

Arati Prakash[1], Benedetta Flebus[2], Jack Brangham[1], Fengyuan Yang[1], Yaroslav Tserkovnyak[2], Joseph P. Heremans[3,1,4]

[1] Department of Physics, The Ohio State University, Columbus, Ohio 43210, USA

[2] Department of Physics and Astronomy, University of California, Los Angeles, California 90095, USA

[3] Department of Mechanical Engineering, The Ohio State University, Columbus, Ohio 43210, USA

[4] Department of Materials Science and Engineering, The Ohio State University, Columbus, Ohio 43210, USA

Abstract

Temperature-dependent spin-Seebeck effect data on Pt|YIG ($Y_3Fe_5O_{12}$)|GGG ($Gd_3Ga_5O_{12}$) are reported for YIG films of various thicknesses. The effect is reported as a spin-Seebeck resistivity (SSR), the inverse spin-Hall field divided by the heat flux, to circumvent uncertainties about temperature gradients inside the films. The SSR is a non-monotonic function of YIG thickness. A diffusive model for magnon transport demonstrates how these data give evidence for the existence of two distinct length scales in thermal spin transport, a spin diffusion length and a magnon energy relaxation length.

Since the discovery of the (longitudinal) spin-Seebeck effect (SSE)[1], much work has been done to identify the length scales involved in the phenomenon.[2] Using nonlocal detection, it has been shown that relaxation of thermal magnons in YIG is governed by a spin diffusion length λ_S.[3] The latter is reported to be around 10 μm, and in some studies increases to up to 70 μm at low temperatures.[4,5] This has led to a consensus that the micron-scale dependence of SSE observed in planar geometries corresponds to the generation and accumulation of the nonequilibrium magnon density gradients in the bulk. It is clear that magnon energy relaxation mechanisms by the phononic environment must be invoked generally for a complete understanding of thermal spin transport, and particularly for the physics underlying the SSE. Indeed, while heaters and thermometers couple to phonons, these must in turn couple to magnons in order to give rise to the SSE in a magnon-based system like YIG. These relaxation processes can be parameterized by the length λ_T over which magnon-to-phonon thermalization occurs,[6] and λ_T is expected to be a much smaller length scale than λ_S; a theoretical argument can be found in Ref. [7]. Several prior attempts were made to quantify λ_T. Multi-parameter fits to spin-Seebeck[5] and spin-Peltier[8] measurements derive a value for λ_T that are up to one order of magnitude shorter than the lattice spacing of YIG (1.237 nm), indicating that the models used do not resolve the difference between magnon and phonon temperatures. Brillouin light scattering measurements of the magnon temperature[9] also do not resolve a difference between magnon and phonon temperature, albeit within an experimental resolution (±4K) that is one to two orders of magnitude larger than the temperature difference across a YIG layer in a classical spin-Seebeck configuration. Phonon-magnon drag has been put into evidence in previous SSE experiments[10,11], which again points to the importance of magnon-phonon interactions, but don't quantify it. Therefore, to the best of our knowledge, other than the fits mentioned above, no experimentally

explicit evidence for the effect of this length scale on SSE measurements has been reported to date. For completeness, we draw attention to the length scale extracted from the heat-pulse measurements in Ref. [12]. While this length scale may be expected to be long and possibly intermediate between λ_T and λ_S, its extraction relies on the coupled heat-spin dynamics near the interface that is associated with innately transient behavior.

Previous articles on thin films using various growth techniques[13,14,15] have shown the SSE signal to increase with increasing YIG film thickness. In this study, we grow a series of Pt|YIG|GGG heterostructures, with YIG thickness varying from 10 nm to 1 μm, using the same growth technique for all films. We measure the temperature-dependent spin-Seebeck effect on these structures and of bulk single-crystal Pt|YIG. The spin-Seebeck signal increases for film thicknesses from 10 to 250 nm and again for the bulk YIG film, but in between, the signal reaches a local maximum at a thickness ~ 250 nm – a detailed comparison with previous studies is underneath.

We explain the non-monotonic behavior in terms of the energy-equilibration dynamics of magnons to phonons in the YIG. We implement a diffusive model for spin and heat transport in order to parametrize magnon-phonon thermal relaxation,[6,7] which allows us to interpret our observations. Using typical material parameters for YIG and values for interfacial thermal conductances of the Pt|YIG|GGG heterostructure from Ref. [16], we calculate thermally driven spin current as a function of the YIG film thickness. In our picture, a local maximum is governed by the magnon energy relaxation length, and the spin current eventually saturates at thicknesses beyond the measured magnon spin diffusion length. Thus, the non-monotonicity is evidence that there are two mechanisms at play, occurring on two different length scales, which define the magnonic spin-Seebeck effect.

A series of YIG films with varied thickness (10 nm, 40 nm, 100 nm, 250 nm, 500 nm, 1 μm) were grown epitaxially on single crystal GGG <100> substrates by ultrahigh-vacuum off-axis sputtering. The growth of the 1 μm-thick film took nearly 2 days; longer growths were not technically feasible because the target conditions cannot be maintained stable over longer periods of growth time. Then, Pt layers of thickness 6 nm were deposited at room temperature on the YIG films, also by off-axis sputtering. A bulk, 500 μm single-crystal YIG <100> substrate was obtained from Princeton Scientific, so that YIG crystal orientation was controlled for all samples. Pt was deposited on this bulk crystal in the manner described for GGG. The quality of the films of all thicknesses used for SSE measurements is verified to be uniform, by vibrating sample magnetometer measurements of the saturation magnetization and by measurements of the ferromagnetic resonance linewidth. The data on the films up to 250 nm thickness are in Refs. [17] and [18]. The supplement reports additional measurements of the saturation magnetization, extending the results to YIG films of 1 μm thickness.[19]

Spin-Seebeck thermopower measurements were conducted at low temperatures from 2 to 300 K on a Physical Property Measurement System (PPMS) by Quantum Design.[20] While the electrical measurements are quite accurate, the measurements of the imposed temperature profile are not, because this quantity must be estimated across the layer of YIG that supports magnon transport. Practical measurements obtain one of two values. First, they may obtain the temperature difference ΔT across the full Pt|YIG|GGG stack, and proportion this somehow across the layers. Second, they may estimate a value for the temperature gradient ∇T from a heat flux measurement combined with a known value of thermal conductivity. Crucially, the estimates of ∇T require knowledge of its variation across the Pt|YIG|GGG stack, which is inaccessible experimentally given the presence of interfacial thermal resistances (Pt|YIG and

YIG|GGG), differences between the thermal conductivities of the different layers, and the fact that the thermal conductivity of the YIG film is not known accurately since it depends on thickness. We show in detail in the supplement[19] how these methods yield inconsistent conclusions. Particularly, the temperature dependence of the experimental results when represented as a spin-Seebeck coefficient (SSC) in thermopower units [μV/K] reflects, in essence, the temperature dependence of the thermal conductivity of bulk YIG or GGG, which is dominated by phonons above 10 K.[21] Further, recent work[22] systematically shows the lack of repeatability and, thus, reliability of this representation of the magnitude of the SSE.

In a proper adiabatic sample mount, the heat flux j_Q (in units of W/m^2) is unidirectional, flows entirely into the sample, and is measured reliably from the knowledge of the sample cross-section and the amount of electrical power dissipated by a resistive heater. Cryostat calibrations show the heat losses to be at most 15 mW/K at 300 K, slightly less than two orders of magnitude lower than the thermal conductance of the sample, so that j_Q is a well-defined experimental quantity by which we can parameterize the spin-Seebeck response.

Circumventing the need to estimate ∇T, we report our data in terms of a spin-Seebeck resistivity (SSR), $R_{SSE} \equiv E_{Pt}/j_Q$ (in units of m/A), as a function of temperature in Figure 1. From these data, we derive the thickness dependence of SSR over a broad temperature range, spanning 20 to 300 K, in Figure 2. The data show two features. The first is the non-monotonic behavior of the thickness dependence of the SSR described above: the signal shows first an increase with increasing thickness up to 250 nm, but is followed by a clearly resolved decrease, leading to a minimum at or slightly above 1 μm. Second, while the data on bulk YIG clearly are dependent

on temperature, those below 1 μm have only a weak dependence. We point out that this feature is seen best when the data are plotted as SSR (per unit heat flux) and less so in the SSC (μV/K).[19]

These results are discussed in the context of the existing literature. Ref. [13] studies thickness dependence of the SSE on two different sample sets: the results suggest a saturation of the SSE signal at 200 nm for the first set, and around 10 μm for the second. Film thicknesses in the pertinent interval (between 200 nm and several microns) are not studied. The data from Ref. [13] are thus broadly consistent with the observations of Fig. 2. The non-monotonicity appears to be absent in Ref. [14] in the relevant thickness range. However, there are rather few data points in that range, and the SSE signals are an order of magnitude lower than those presented here (in units of μV/K in the supplement[19]) so that the amplitude falls quite close to the apparent resolution in Ref. [14]. These factors would make it difficult to resolve the local maximum reported in Fig. 2. Finally, in Ref [15], which uses a different measurement method, the thickness dependence of the SSE voltage shows one outlying data point at 200 nm, which corresponds rather well to the observation in Fig. 2. This point also deviates from the model, which is based on only a magnon diffusion length. In fact, the discussion in Ref [15] concludes that the local SSE may be governed by a length scale different from the magnon diffusion length that is extracted from nonlocal signals. From this comparison to the literature, it appears that Fig. 2 offers insight to such a length scale, by adding data points in the relevant YIG thickness range.

We model the experiment by considering the one-dimensional geometry shown in Fig. 3. The experimentally controlled heat flux defines the phonon temperature gradient $\partial_x T_p < 0$ in YIG. We treat phonon transport as diffusive, and we assume that the phonon temperature in the YIG, T_p, is not perturbed significantly by the magnons. The temperature drops at the left interface, $\delta T_L = T_{p,L} - T_p(0)$, and at the right, $\delta T_R = T_p(d) - T_{p,R}$, with $T_{p,L(R)}$ being the

phonon temperature in Pt (GGG), can then be determined by solving the phonon heat-diffusion equation[16]:

$$\delta T_{L(R)} = -\ell_{L(R)}\, \partial_x T_p\,. \tag{1}$$

Here, we have introduced the Kapitza length of the Pt(GGG)|YIG interface as $\ell_{L(R)} = \kappa_p / \mathrm{K}_{p,L(R)}$, where κ_p is YIG phonon thermal conductivity and $\mathrm{K}_{p,L(R)}$ the phonon interfacial thermal conductance for the Pt(GGG)|YIG interface.

In YIG, scattering processes among thermal magnons, which are governed by exchange interactions, occur on a much shorter timescale than magnon lifetime. Magnons are assumed to remain in a thermal distribution, which is then described by a magnon temperature $T_m(x)$ and an effective magnon chemical potential $\mu(x)$[5,23] that parametrize the non-equilibrium distribution induced by the thermal bias. Treating transport semi-classically, the magnon spin- and heat-continuity equations read as[7]

$$\partial_t n + \partial_x j = -g_{n\mu}\,\mu - g_{nT}\left(T_m - T_p\right), \tag{2a}$$

$$\partial_t u + \partial_x q = -g_{uT}\left(T_m - T_p\right) - g_{u\mu}\,\mu\,, \tag{2b}$$

where n is the density of the thermal magnons and u the energy density carried by them. The $g_{n\mu}$ and $g_{u\mu}$ coefficients account for the relaxation by phononic environment of magnon spin and temperature, respectively. The cross-terms g_{nT} and g_{uT} describe the generation or decay of spin accumulation by heating or cooling of magnons and vice versa, and are related by the Onsager-Kelvin relation, i.e., $T_m\, g_{nT} = g_{u\mu}$. In the linear response regime and neglecting magnon-phonon drag contributions $j\,, q \propto \partial_x T_p$ (restoring phonon drag would simply rescale the

bulk bias terms proportional to $\partial_x T_p$), the spin, j, and heat, q, currents carried by magnons can be written as

$$j = -\sigma \partial_x \mu - \zeta \partial_x T_m, \tag{3a}$$

$$q = -\kappa \partial_x T_m - \varrho \partial_x \mu, \tag{3b}$$

where σ, κ, ζ, and $\varrho = T_m\ \zeta$ are the bulk spin and heat conductivities and the intrinsic spin Seebeck and Peltier coefficients, respectively.

Equations (2a) and (2b) must be determined consistently with the boundary conditions for spin and heat transport at the Pt|YIG and YIG|GGG interfaces. For Pt|YIG, at $x = 0$, the latter reads as

$$j = -G_L\ \mu + S_L\ \delta T_L + S_L(T_p - T_m), \tag{4a}$$

$$q = K_L\ \delta T_L + K_L\ (T_p - T_m) - \Pi_L\ \mu, \tag{4b}$$

where G_L, K_L, S_L, and $\Pi_L = T_m S_L$ are the interfacial magnon spin and thermal conductances and spin-Seebeck and Peltier coefficients, respectively. Note that the spin current (4a) injected at the Pt|YIG interface is directly proportional to the measurable inverse spin-Hall voltage.[24]

At the YIG|GGG interface, the spin flow is blocked as there are no spin carriers in the GGG substrate. Nevertheless, heat still can be transmitted via inelastic spin-preserving scattering processes between magnons and phonons. The corresponding boundary conditions at $x = d$ can be written as:

$$j = 0, \tag{5a}$$

$$q = K_R\,\delta T_R - K_R\ \ (T_p - T_m). \tag{5b}$$

Here, K_R is the interfacial magnon heat conductance, which accounts for the processes leading to energy exchange between magnons and phonons at the YIG|GGG interface. The interfacial magnon spin conductance G_R, the spin Seebeck S_R, and, consequently, the spin-Peltier coefficient $\Pi_R = T_m S_R$,vanish.

Next we introduce the magnon energy relaxation length, $\lambda_T = \sqrt{\kappa/g_{uT}}$, and the spin diffusion length, $\lambda_s = \sqrt{\sigma/g_{n\mu}}$, which parametrize the relaxation of the magnon temperature to the phonon temperature and the relaxation of the magnon chemical potential to its equilibrium (vanishing) value, respectively. Since the spin-preserving relaxation of magnon distribution towards the phonon temperature does not rely on relativistic spin-orbit interactions, the associated length scale λ_T can be taken to be much shorter than the spin diffusion length λ_s.[5,7,25]

Based on the latter assumption, we identify two distinct transport regimes as functions of the thickness d of the YIG. When the thickness is comparable or larger than the spin diffusion length, i.e., $d \geq \lambda_s \gg \lambda_T$, we assume the transport to be dominated by the mechanisms leading to the relaxation of the magnon chemical potential, while setting $T_p = T_m$ throughout the YIG.[19] As shown in Figure 4, the corresponding contribution to the injected current at the Pt|YIG interface grows monotonically as function of the YIG thickness, ultimately to saturate for large thicknesses. The underlying physical picture is clear. The temperature bias induces a chemical potential imbalance at the left interface. The corresponding magnon density increases with increasing sample thickness. However, when $d \gg \lambda_s$, magnons will decay – via non-spin-preserving interactions with the lattice – before reaching the left end of the sample, and the SSE signal will not increase further.

In the opposite regime, when $d \sim \lambda_T << \lambda_S$, we disregard instead any chemical-potential imbalance (i.e, by setting $\mu = 0$). In this case, the relaxation of the magnon temperature to the phonon temperature emerges as a driving mechanism for transport. In order to analyze the corresponding contribution to the injected spin current, we treat the magnon heat Kapitza length $\ell^*_{T,R} = \kappa/K_R$ at the YIG|GGG interface as a free parameter, as there is no current estimate for interfacial thermal conductance K_R. Estimates for the other length scales can be found in the supplement.[19] Figure 5 shows that we reproduce a non-monotonic behavior of the injected spin current for $\ell^*_{T,R} \ll \ell^*_{T,L}, \lambda_T$. To understand this result, recall that the magnon heat Kapitza length $\ell^*_{T,R}$ parametrizes the strength of spin-preserving inelastic interactions between magnons in YIG and phonons at GGG at the right interface; in other words, a short $\ell^*_{T,R}$ corresponds to an efficient thermalization process. As the phonon temperature in the GGG substrate $T_{p,L(R)}$ is lower than that in the YIG, i.e., $\delta T_R > 0$, thermalization mechanisms between magnons in YIG and phonons in GGG lower the magnon temperature T_m near the YIG|GGG interface over a shorter timescale than the one governing the thermalization of magnons and phonons in YIG. Hence, the right interface acts as a source of "cold" magnons, which contribute positively to the temperature imbalance in YIG, $T_p - T_m$. However, when the sample thickness is larger than the temperature relaxation length λ_T, these magnons thermalize with phonons before reaching the left interface. Thus, for $d > \lambda_T$, the YIG|GGG interface no longer acts as an effective source for the magnon-phonon temperature imbalance in YIG, leading to the non-monotonicity observed in Figure 5. We suggest that this theoretical feature is related to our experimental observations, and imply that the thickness at which the peak in SSR versus YIG thickness emerges is in direct correspondence with the magnon energy relaxation length in YIG, leading to an experimental estimate of the latter as $\lambda_T \sim 250$ nm.

Relating the experimental peak to the magnon energy relaxation length scale allows us to interpret the weak temperature dependence of the SSR measurements as the little-to-none temperature dependence of the magnon energy relaxation length. While surprising at first, the apparent lack of temperature dependence of λ_T shown in Figure 2 parallels that reported for the spin diffusion length λ_s [3]. Additionally, although the microscopic origin of λ_s relies on spin-relaxing interactions, whereas the magnon energy relaxation length λ_T is in our analysis introduced as a spin-preserving interaction, it may be interesting to compare the weak temperature dependence of λ_T to the rather weak temperature dependence of the Gilbert damping parameter.[26,27] Notwithstanding these remarks, the weakness of the temperature dependence of λ_T is an issue that should be investigated in the future.

In summary, our data and model suggest that the measured dependence of the SSR on the sample thickness reflects magnon spin and heat diffusion processes occurring on separate length scales. We show how a non-monotonic feature in the signal observed at short thicknesses can emerge corresponding to the length scale parametrizing magnon-phonon thermalization mechanisms, and we offer an estimate for the latter, i.e., $\lambda_T \sim 250$ nm. While a diffusive approach to the magnon heat transport qualitatively captures the newly observed feature, here we want to stress that our model represents a concept, rather than a complete theory of transport at short thicknesses. Future work should address the nonequilibrium mechanisms operating over such length scales beyond the diffusive approximation rigorously.

Acknowledgement

This work was supported primarily by the Center for Emergent Materials, an NSF MRSEC, grant DMR-1420451 and the Army Research Office (ARO) MURI W911NF-14-1-0016 and the U.S. Department of Energy (DOE), Office of Science, Basic Energy Sciences, grant No. DE-SC0001304. Additional funding for the theoretical work is from the European Research Council, and the D-ITP consortium, a program of the Netherlands Organization for Scientific Research (NWO) that is supported by the Dutch Ministry of Education, Culture and Science (OCW).

Figure Captions

Figure 1. Temperature dependence of the SSR for various YIG film thicknesses and bulk YIG.

Figure 2. Thickness dependence of the SSR at the various temperatures indicated on the graph.

Figure 3. Qualitative illustration of the phonon temperature profile in a Pt|YIG|GGG heterostructure.

Figure 4. Thickness dependence of the spin current injected at the Pt|YIG interface in the far regime, i.e. where the thickness is represented on the scale of the magnon spin diffusion length λ_S. Here, spin transport is dominated by the mechanisms leading to relaxation of the magnon chemical potential. The spin current is normalized by the thermal spin current in the bulk $j_{s,q} = -\zeta \partial_x T_p$.

Figure 5. Thickness dependence of the spin current injected at the Pt|YIG interface in the near regime, i.e., where the thickness is represented on the scale of the magnon energy relaxation length λ_T. Here, the chemical-potential imbalance is disregarded, and the non-monotonicity results from the interplay between λ_T and the presence of cold magnons at the YIG|GGG interface. The spin current is normalized by the thermal spin current in the bulk $j_{s,q} = -\zeta \partial_x T_p$.

References

[1] K. Uchida, H. Adachi, T. Ota, H. Nakayama, S. Maekawa, and E. Saitoh, Appl. Phys. Lett. **97**, 172505 (2010).

[2] S. Hoffman, K. Sato, and Y. Tserkovnyak, Phys. Rev. B **88,** 064408 (2013).

[3] L.J. Cornelissen, J. Liu, R.A. Duine, J. Ben Youssef, and B.J. van Wees, Nature Physics **11**, 10221026 (2015).

[4] B. Giles, Z. Yang, J.S. Jamison, and R.C. Myers, Phys. Rev. B **92**, 224415, (2015).

[5] L.J. Cornelissen, K.J.H. Peters, G.E.W. Bauer, R.A. Duine, and B.J. van Wees, Phys. Rev. B **94,** 014412 (2016).

[6] D.J. Sanders and D. Walton, Phys. Rev. B **15,** 1489 (1977).

[7] B. Flebus, S.A. Bender, Y. Tserkovnyak, and R.A. Duine, Phys. Rev. Lett. **116,** 117201 (2016).

[8] J. Flipse, F.K. Dejene, D. Wagenaar, G.E.W. Bauer, J. Ben Youssef, and B.J. van Wees, Phys. Rev. Lett. **113**, 027601 (2014).

[9]M. Agrawal, V.I. Vasyuchka, A.A. Serga, A.D. Karenowska, G.A. Melkov, and B. Hillebrands, Phys. Rev. Lett. **111**, 107204 (2013).

[10] C.M. Jaworski, J. Yang, S. Mack, D.D. Awschalom, R.C. Myers, and J.P. Heremans, Phys. Rev. Lett. **106**, 186601 (2011).

[11] H. Adachi, K. Uchida, E. Saitoh, J. Ohe, S. Takahashi, S. Maekawa, Appl. Phys. Lett. **97**, 252506 (2010).

[12] M. Agrawal, V.I. Vasyuchka, A.A. Serga, A. Kirihara, P. Pirro, T. Langner, M.B. Jungfleisch, A.V. Chumak, E.Th. Papaioannou, and B. Hillebrands, Phys. Rev. B **89**, 224414 (2014).

[13] A. Kehlberger, et al., Phys. Rev. Lett. **115,** 096602 (2015).

[14] E-J. Guo, J. Cramer, A. Kehlberger, C.A. Ferguson, D.A. MacLaren, G. Jakob, M. Kläui, Phys. Rev. X **6**, 031012 (2016).

[15] J. Shan, L.J. Cornelissen, N. Vlietstra, J. B. Youssef, T. Kuschel, R.A. Duine, B.J. van Wees. Phys. Rev. B **94**, 174437 (2016).

[16] M. Schreier, A. Kamra, M. Weiler, J. Xiao, G.E.W. Bauer, R. Gross, and S.T.B. Goennenwein, Phys. Rev. B **88**, 094410 (2013).

[17] J.C. Gallagher, et al. Appl. Phys. Lett. **109**, 072401 (2016).

[18] C.L. Jermain, et al. Phys. Rev. B **95**, 174411 (2017).

[19] See Supplemental Material at [URL will be insterted by publisher] for (a) the results of the main text but now plotted in the more conventional way as the ratio of the spin-Seebeck signal divided by the temperature gradient rather than plotted as in the main text; (b) the sample magnetization data, used to characterize the quality of the samples; (c) the detailed algebraic derivation of the transport theory, the results of which are summarized in the main text.

[20] A. Prakash, J. Brangham, F. Yang, and J.P. Heremans, Phys. Rev. B **94**, 014427 (2016).

[21] S.R. Boona and J.P. Heremans, Phys. Rev. B **90,** 064421 (2014).

[22] A. Sola, P. Bougiatioti, M. Kuepferling, D. Meier, G. Reiss, M. Pasquale, T. Kuschel, and V. Basso, Sci. Rep. **7**, 46752 (2017).

[23] C. Du, et al. arXiv:1611.07408 [cond-mat.mes-hall] (2016).

[24] J. Xiao, G.E.W. Bauer, K. Uchida, E. Saitoh, S. Maekawa, Phys. Rev. B **81**, 214418 (2010).

[25] B. Flebus, K. Shen, T. Kikkawa, K. Uchida, Z. Qiu, E. Saitoh, R.A. Duine, and G.E.W. Bauer, Phys. Rev. B **95,** 144420 (2017).

[26] M. Sparks, Ferromagnetic-Relaxation Theory. McGraw-Hill, New York, page 161.

[27] H. Maier-Flaig, et al. Phys. Rev. B **95**, 214423 (2017).

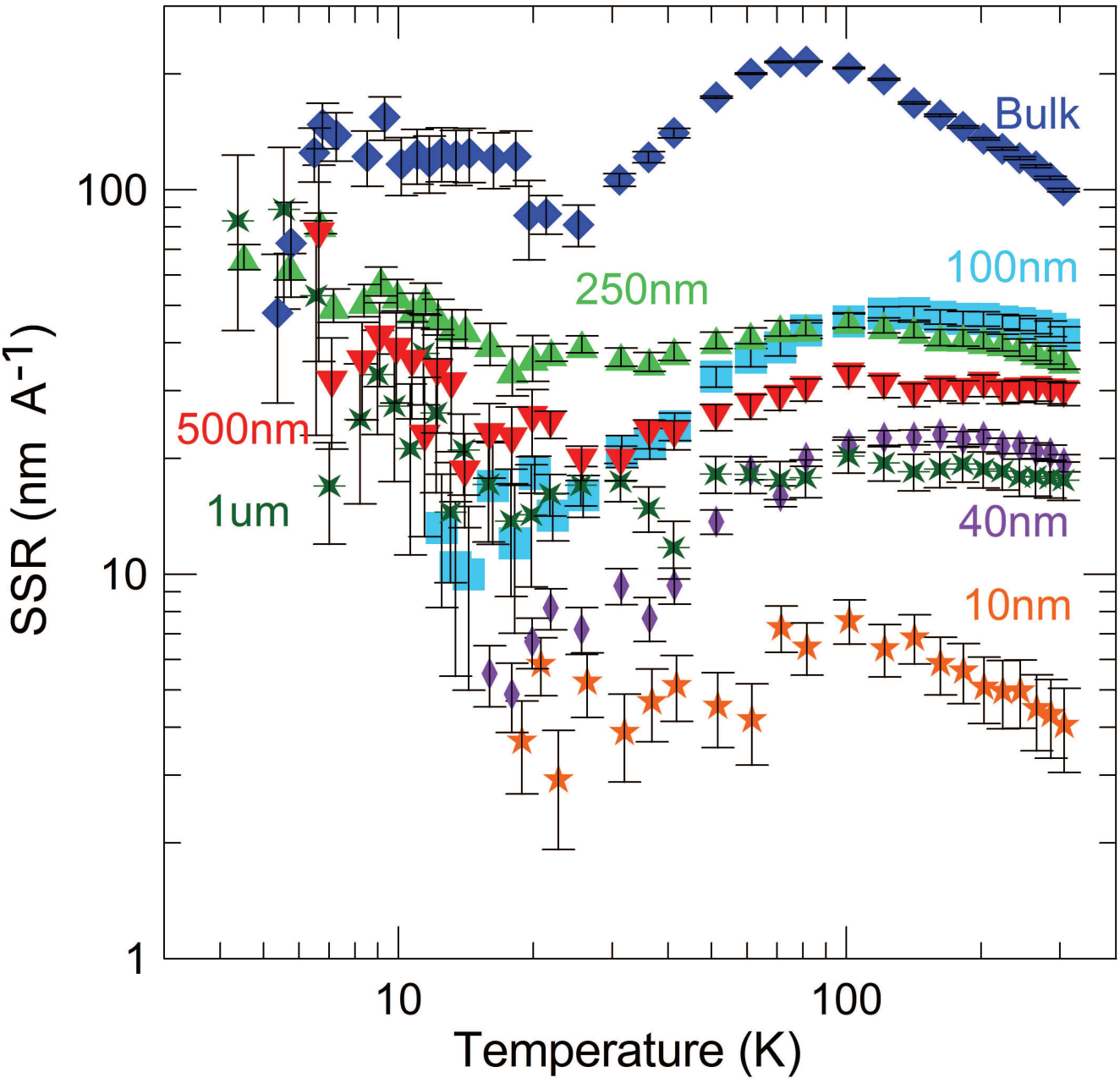

Figure 1 LF16738 19DEC2017

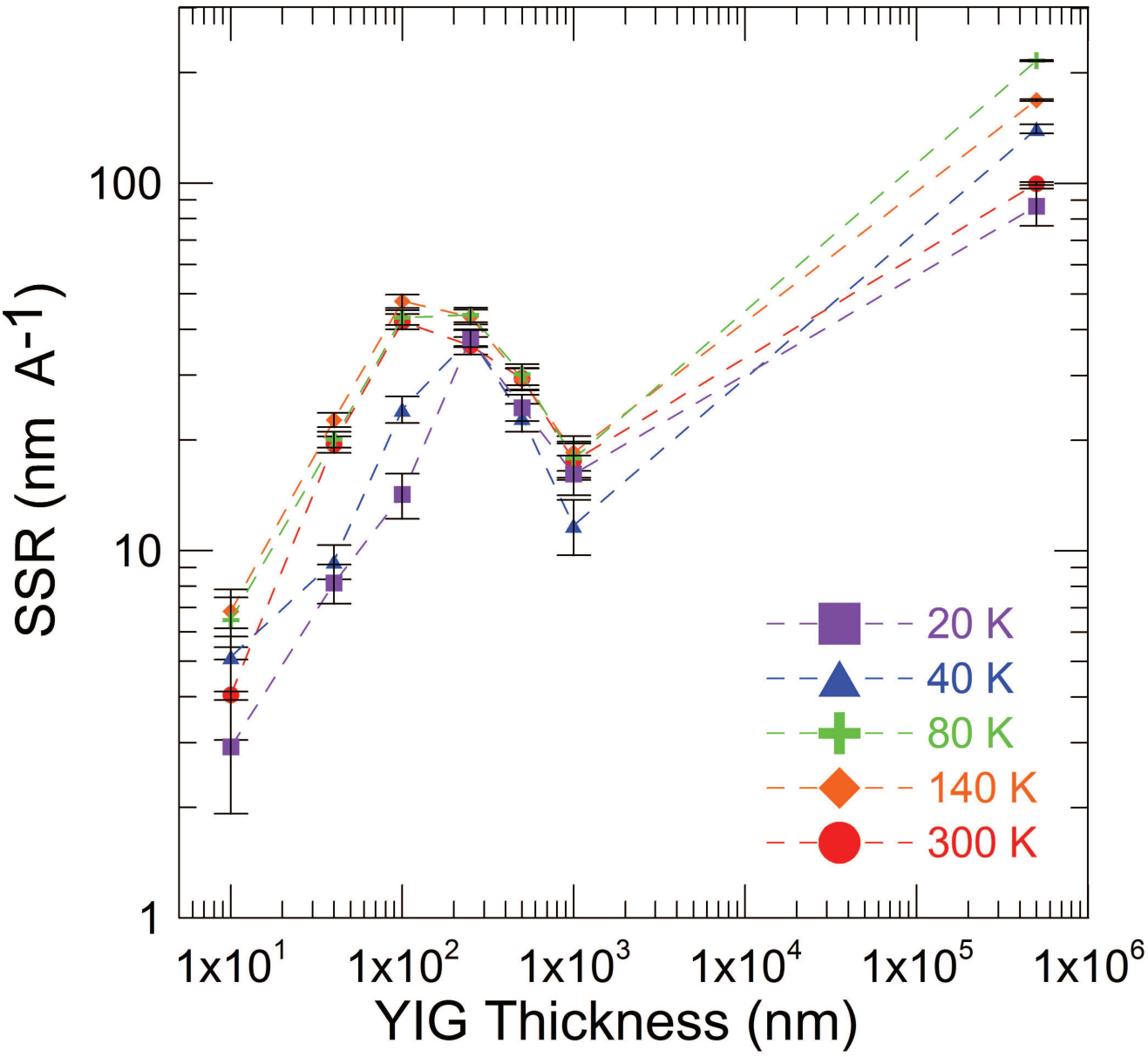

Figure 2 LF16738 19DEC2017

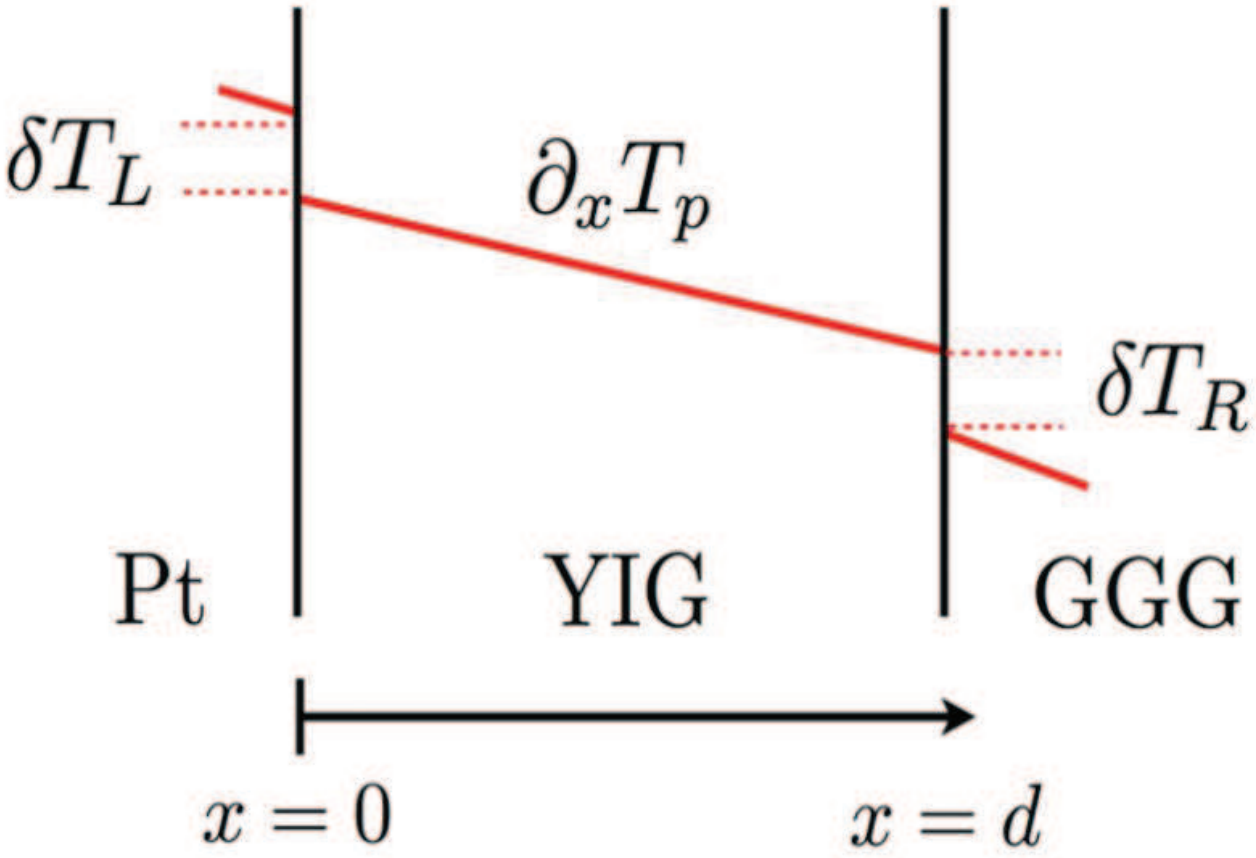

Figure 3 LF16738 19DEC2017

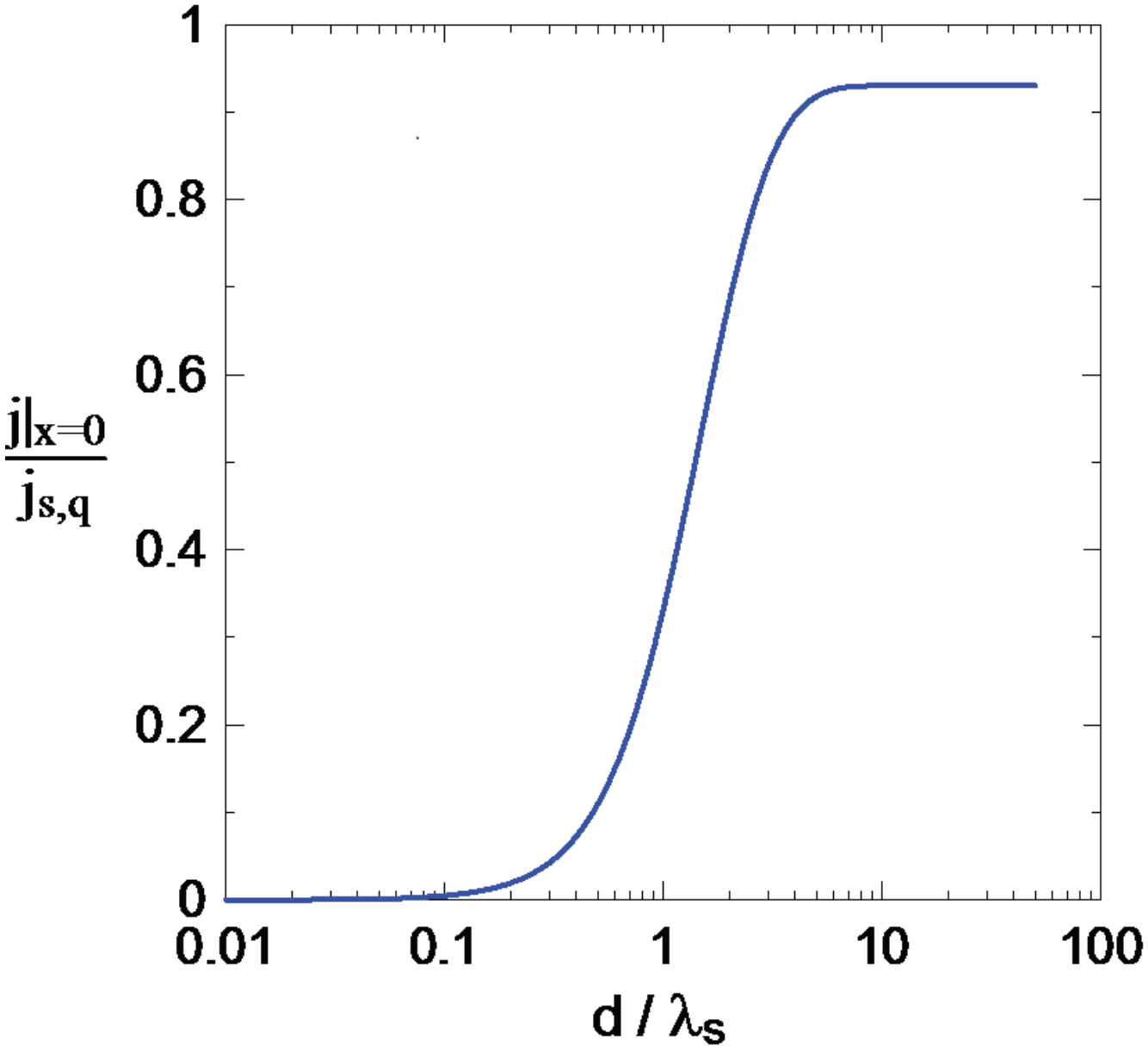

Figure 4 LF16738 19DEC2017

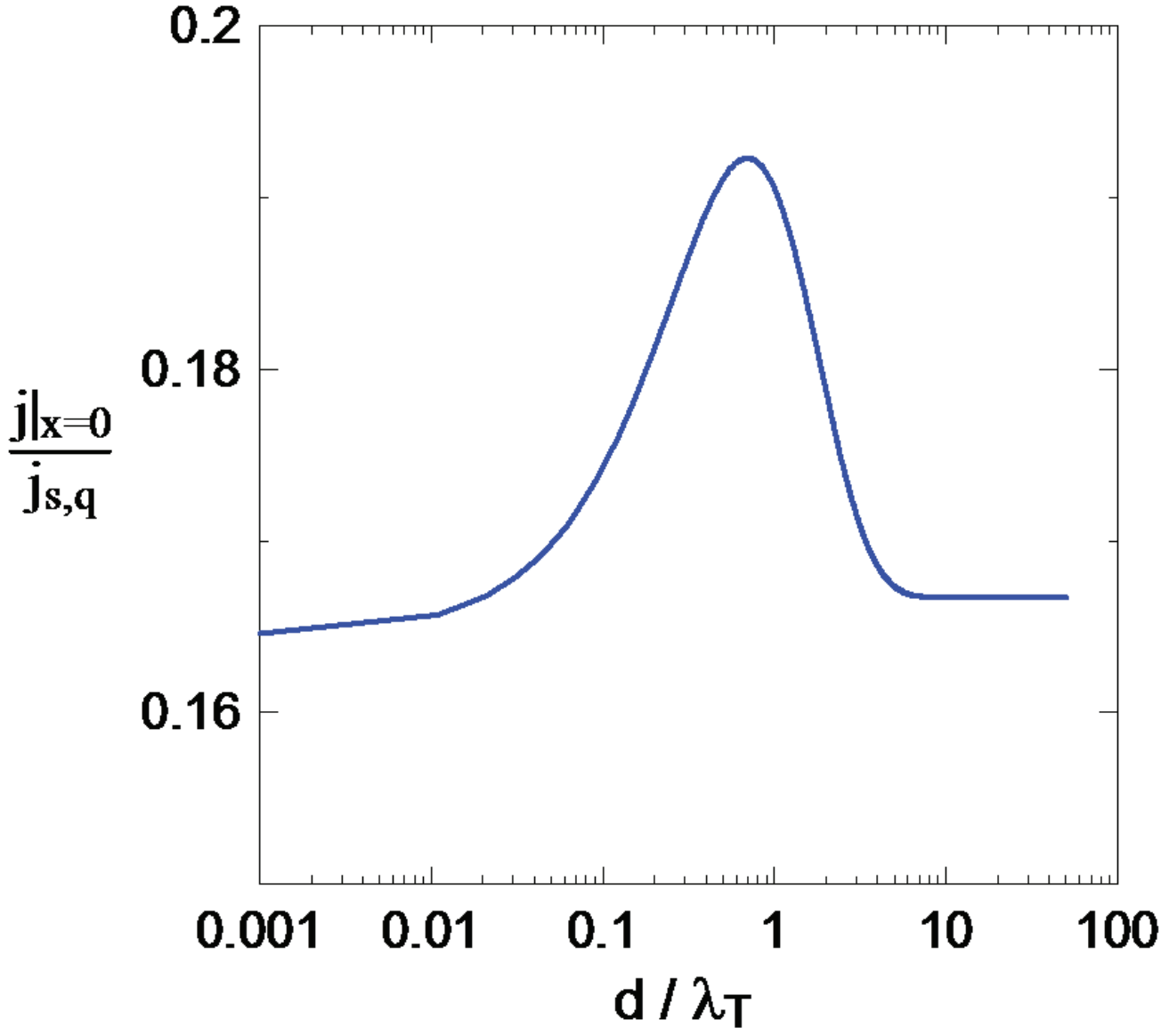

Figure 5 LF16738 19DEC2017